CERN-PH-TH/2008-167
SI-HEP-2008-15

Precision Physics with $B_s^0 \to J/\psi\phi$ at the LHC: The Quest for New Physics

Sven Faller,[a,b] Robert Fleischer[a,c] and Thomas Mannel[a,b]

[a] *Theory Division, Department of Physics, CERN, CH-1211 Geneva 23, Switzerland*

[b] *Theoretische Physik 1, Fachbereich Physik, Universität Siegen, D-57068 Siegen, Germany*

[c] *Dipartimento di Fisica, Università di Roma "La Sapienza", I-00185 Roma, Italy*

Abstract

CP-violating effects in the time-dependent angular distribution of the $B_s^0 \to J/\psi[\to \ell^+\ell^-]\phi[\to K^+K^-]$ decay products play a key rôle for the search of new physics. The hadronic Standard-Model uncertainties are related to doubly Cabibbo-suppressed penguin contributions and are usually assumed to be negligibly small. In view of recent results from the Tevatron and the quickly approaching start of the data taking at the LHC, we have a critical look at the impact of these terms, which could be enhanced through long-distance QCD phenomena, and explore the associated uncertainty for the measurement of the CP-violating B_s^0–$\bar{B}_s^0$ mixing phase. We point out that these effects can actually be controlled by means of an analysis of the time-dependent angular distribution of the $B_s^0 \to J/\psi[\to \ell^+\ell^-]\bar{K}^{*0}[\to \pi^+K^-]$ decay products, and illustrate this through numerical studies. Moreover, we discuss $SU(3)$-breaking effects, which limit the theoretical accuracy of our method, and suggest internal consistency checks of $SU(3)$.

October 2008

1 Introduction

The exploration of CP-violating effects in B_s-meson decays offers a particularly promising probe for the search of New Physics (NP). In this respect, a key channel is $B_s^0 \to J/\psi\phi$, which is the counterpart of the "golden" decay $B_d^0 \to J/\psi K_S$ to measure the angle β in the unitarity triangle (UT) of the Cabibbo–Kobayashi–Maskawa (CKM) matrix. Since the $B_s^0 \to J/\psi\phi$ decay involves two vector mesons in the final state, the time-dependent angular distribution of the decay products of the vector mesons, $J/\psi \to \ell^+\ell^-$ and $\phi \to K^+K^-$, has to be measured in order to disentangle the admixture of different CP eigenstates [1, 2].

Within the Standard Model (SM), the CP-violating effects in the time-dependent $B_s^0 \to J/\psi\phi$ angular distribution are expected to be small. On the other hand, a preferred mechanism to accommodate a measurement of non-vanishing CP asymmetries would be given by CP-violating NP contributions to B_s^0–$\bar{B}_s^0$ mixing (see, for instance, [3]). Recent results from the first tagged, time-dependent $B_s^0 \to J/\psi\phi$ analyses performed by the CDF [4] and DØ [5] collaborations at the Tevatron (FNAL) may actually point towards this direction, and have led to quite some attention [6]. The $B_s^0 \to J/\psi\phi$ decay is a main target of the LHCb experiment (CERN), which will soon start taking data and will allow us to explore the CP-violating phenomena in this transition with impressive accuracy [7]: already with $2\,\text{fb}^{-1}$ of data, corresponding to one nominal year of operation, the experimental uncertainty for the B_s^0–$\bar{B}_s^0$ mixing phase ϕ_s is expected to be $\sigma(\phi_s)_{\text{exp}} \sim 1^\circ$, and an upgrade of LHCb with an integrated luminosity of $100\,\text{fb}^{-1}$ would eventually allow us to even reach a sensitivity of $\sigma(\phi_s)_{\text{exp}} \sim 0.2^\circ$ [8].

In view of these exciting prospects, we have a closer look at the CP-violating effects in the time-dependent $B_s^0 \to J/\psi[\to \ell^+\ell^-]\phi[\to K^+K^-]$ angular distribution that arise within the SM and limit the theoretical accuracy of the benchmark for the search for NP. Here the key rôle is played by penguin topologies, which are doubly Cabibbo suppressed and hence usually assumed to be negligible. However, these contributions cannot be calculated reliably from QCD, and could mimic CP-violating effects which might be misinterpreted as signals of NP in B_s^0–$\bar{B}_s^0$ mixing with a small but sizeable CP-violating NP phase.

In the present paper, we point out that the penguin effects can actually be controlled by means of an analysis of the angular distribution of $B_s^0 \to J/\psi[\to \ell^+\ell^-]\bar{K}^{*0}[\to \pi^+K^-]$ and its CP conjugate. Applying $SU(3)$ flavour-symmetry arguments and neglecting penguin annihilation and exchange topologies (which can be probed through $B_d^0 \to J/\psi\phi$), the relevant hadronic parameters entering the $B_s^0 \to J/\psi\phi$ observables can be deter-

mined, thereby allowing us to take them into account in the extraction of ϕ_s. We suggest to perform a simultaneous analysis of the $B_s^0 \to J/\psi\phi$ and $B_s^0 \to J/\psi\bar{K}^{*0}$ channels at LHCb, and encourage the CDF and DØ collaborations to search for signals of this transition, as these would allow us to give first constraints on the penguin effects in $B_s^0 \to J/\psi\phi$ and their impact on the extraction of the CP-violating B_s^0–$\bar{B}_s^0$ mixing phase. Further information can be obtained from the $B_d^0 \to J/\psi\rho^0$ decay, in particular for the resolution of a discrete ambiguity through experimental data.

As pointed out in Ref. [9], the data for CP violation in $B_d^0 \to J/\psi\pi^0$ and the branching ratio of this channel signal that such effects are sizeable and soften the tension in the fit of the UT between its angle β and side R_b as determined through CP violation in $B_d^0 \to J/\psi K_{\rm S,L}$ decays and semileptonic $b \to u, c$ transitions, respectively. In particular, the measurement of β has already reached a level of precision where subleading effects, i.e. doubly Cabibbo-suppressed penguin contributions, have to be included in order to match the experimental accuracy (see also Ref. [10]). This feature strengthens the need to deal with such effects in analyses of CP violation in $B_s^0 \to J/\psi\phi$ as well. In particular, we expect that the penguin effects interfere constructively with mixing-induced CP violation and could lead to CP asymmetries as large as $\mathcal{O}(-10\%)$, which would be significantly larger than the naive SM estimate of $\sin\phi_s^{\rm SM} \approx -3\%$ and could be well detected at LHCb.

The outline of this paper is as follows: in Section 2, we give an overview of the $B_s^0 \to J/\psi[\to \ell^+\ell^-]\phi[\to K^+K^-]$ analysis and explore the impact of the penguin effects on the measurement of ϕ_s, while we discuss the strategy to include the hadronic penguin contributions with the help of $B_s^0 \to J/\psi\bar{K}^{*0}$ in Section 3. This strategy is illustrated in Section 4. A detailed discussion of $SU(3)$-breaking effects and internal consistency checks that are offered by the observables of our decays into two vector mesons are given in Section 5. Finally, we summarize our conclusions in Section 6.

2 Review of $B_s^0 \to J/\psi\phi$

2.1 Structure of the Angular Distribution

In contrast to the decay $B_d^0 \to J/\psi K_{\rm S}$, we have to deal with two vector mesons in the final state of $B_s^0 \to J/\psi\phi$, which is an admixture of CP-odd and CP-even eigenstates. Using the angular distribution of the decay products of the vector mesons, the CP eigenstates can be disentangled. To this end, we introduce linear polarization states of the vector mesons, which

are longitudinal (0) or transverse to their directions of motion. In the latter case, the polarization states may be parallel ($\|$) or perpendicular ($\perp$) to one another [11]. The time-dependent angular distribution of $B_s^0 \to J/\psi\phi$ takes the following general form [1]:

$$f(\Theta, \Phi, \Psi; t) = \sum_k g^{(k)}(\Theta, \Phi, \Psi)\, b^{(k)}(t), \tag{1}$$

where the decay kinematics is described by the $g^{(k)}(\Theta, \Phi, \Psi)$, and the time-dependent coefficients $b^{(k)}(t)$ are given as

$$\begin{gathered} |A_f(t)|^2 \quad (f \in \{0, \|, \perp\}), \\ \mathrm{Re}\{A_0^*(t) A_\|(t)\}, \quad \mathrm{Im}\{A_f^*(t) A_\perp(t)\} \quad (f \in \{0, \|\}), \end{gathered} \tag{2}$$

with linear polarization amplitudes $A_f = \langle (J/\psi\phi)_f | \mathcal{H}_{\rm eff} | B_s^0(t) \rangle$, where $\mathcal{H}_{\rm eff}$ is the relevant low-energy effective Hamiltonian. Here $A_\perp(t)$ describes a CP-odd final-state configuration, whereas $A_0(t)$ and $A_\|(t)$ correspond to CP-even final-state configurations.

In the case of the CP-conjugate decay $\bar{B}_s^0 \to J/\psi\phi$, we may write the angular distribution as

$$\bar{f}(\Theta, \Phi, \Psi; t) = \sum_k \bar{\mathcal{O}}^{(k)}(t) g^{(k)}(\Theta, \Phi, \Psi). \tag{3}$$

Since the meson content of the $J/\psi\phi$ state is the same whether it results from the B_s^0 or $\bar{B}_s^0$ decays, we may use the same angles Θ, Φ and Ψ as in (1) to describe the kinematics of the decay products. Following these lines, the effects of CP transformations relating $B_s^0 \to (J/\psi\phi)_f$ to $\bar{B}_s^0 \to (J/\psi\phi)_f$ are then taken into through the CP eigenvalues of the final-state configuration $(J/\psi\phi)_f$. Therefore the same functions $g^{(k)}(\Theta, \Phi, \Psi)$ are present in (1) and (3). For the explicit form the of these quantities, see Ref. [1].

2.2 Structure of the Decay Amplitudes

As can be seen in Fig. 1, colour-suppressed tree-diagram-like and penguin topologies contribute to the $B_s^0 \to J/\psi\phi$ decay within the SM. For a given final-state configuration $f \in \{0, \|, \perp\}$, the $B_s^0 \to J/\psi\phi$ decay amplitude can therefore be written as

$$A(B_s^0 \to (J/\psi\phi)_f) = \lambda_c^{(s)} \left[A_{\rm T}^{(c)f} + A_{\rm P}^{(c)f} \right] + \lambda_u^{(s)} A_{\rm P}^{(u)f} + \lambda_t^{(s)} A_{\rm P}^{(t)f}, \tag{4}$$

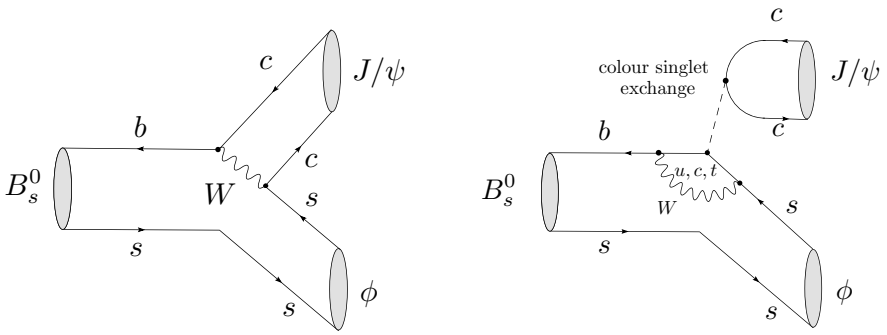

Figure 1: Decay topologies contributing to $B_s^0 \to J/\psi\phi$ in the SM.

where the $\lambda_j^{(s)} \equiv V_{js}V_{jb}^*$ are CKM factors, while $A_{\rm T}^{(c)f}$ and $A_{\rm P}^{(j)f}$ are CP-conserving strong amplitudes related to tree-diagram-like and penguin topologies (with internal $j \in \{u,c,t\}$ quarks), respectively. Using the appropriate low-energy effective Hamiltonian, the latter quantities can be expressed in terms of linear combinations of perturbatively calculable Wilson coefficient functions and non-perturbative hadronic matrix elements of the corresponding four-quark operators, which are associated with large uncertainties. Using the CKM unitarity relation $\lambda_t^{(s)} = -\lambda_c^{(s)} - \lambda_u^{(s)}$ to eliminate the $\lambda_t^{(s)}$ factor, we obtain

$$A(B_s^0 \to (J/\psi\phi)_f) = \left(1 - \frac{\lambda^2}{2}\right) \mathcal{A}_f \left[1 + \epsilon a_f e^{i\theta_f} e^{i\gamma}\right], \tag{5}$$

where

$$\mathcal{A}_f \equiv \lambda^2 A \left[A_{\rm T}^{(c)f} + A_{\rm P}^{(c)f} - A_{\rm P}^{(t)f}\right] \tag{6}$$

and

$$a_f e^{i\theta_f} \equiv R_b \left[\frac{A_{\rm P}^{(u)f} - A_{\rm P}^{(t)f}}{A_{\rm T}^{(c)f} + A_{\rm P}^{(c)f} - A_{\rm P}^{(t)f}}\right] \tag{7}$$

are CP-conserving hadronic parameters, while

$$\lambda \equiv |V_{us}| = 0.22521 \pm 0.00083, \tag{8}$$

$$A \equiv |V_{cb}|/\lambda^2 = 0.809 \pm 0.026, \tag{9}$$

$$R_b \equiv (1 - \lambda^2/2)|V_{ub}/(\lambda V_{cb})| = 0.423^{+0.015}_{-0.022} \pm 0.029, \tag{10}$$

$$\epsilon \equiv \lambda^2/(1-\lambda^2) = 0.053 \tag{11}$$

are CKM parameters [9, 12], and the UT angle γ flips its sign when considering CP-conjugate processes:

$$A(\bar{B}_s^0 \to (J/\psi\phi)_f) = \eta_f \left(1 - \frac{\lambda^2}{2}\right) \mathcal{A}_f \left[1 + \epsilon a_f e^{i\theta_f} e^{-i\gamma}\right]. \tag{12}$$

Here η_f is the CP eigenvalue of the final-state configuration $(J/\psi\phi)_f$.

2.3 Time-dependent Observables

If we neglect CP violation in B_s^0–$\bar{B}_s^0$ oscillations, which can be probed through wrong-charge lepton asymmetries and is a tiny effect in the SM, the formalism of B_s^0–$\bar{B}_s^0$ mixing yields the following expressions [13]:

$$\Gamma[f,t] \equiv |A_f(t)|^2 + |\overline{A}_f(t)|^2 = R_{\rm L}^f\, e^{-\Gamma_{\rm L}^{(s)}t} + R_{\rm H}^f\, e^{-\Gamma_{\rm H}^{(s)}t}, \tag{13}$$

$$|A_f(t)|^2 - |\overline{A}_f(t)|^2 = 2\, e^{-\Gamma_s t}\left[A_{\rm D}^f \cos(\Delta M_s t) + A_{\rm M}^f \sin(\Delta M_s t)\right], \tag{14}$$

where $\Gamma_{\rm L}^{(s)}$ and $\Gamma_{\rm H}^{(s)}$ are the decay widths of the "light" and "heavy" B_s mass eigenstates, respectively, Γ_s is their average, and $\Delta M_s \equiv M_{\rm H}^{(s)} - M_{\rm L}^{(s)}$ the difference of the mass eigenvalues. The labels "D" and "M" remind us that non-vanishing values of $A_{\rm D}^f$ and $A_{\rm M}^f$ are generated through direct and mixing-induced CP-violating effects, respectively.

Since the hadronic parameters $a_f e^{i\theta_f}$, which are essentially unknown, enter (5) and (12) in combination with the doubly Cabibbo-suppressed parameter ϵ, they are usually neglected. In this limit, we obtain

$$\Gamma[f,t] = |\mathcal{N}_f|^2 \left[(1+\eta_f\cos\phi_s)e^{-\Gamma_{\rm L}^{(s)}t} + (1-\eta_f\cos\phi_s)e^{-\Gamma_{\rm H}^{(s)}t}\right], \tag{15}$$

$$|A_f(t)|^2 - |\overline{A}_f(t)|^2 = 2\eta_f|\mathcal{N}_f|^2 e^{-\Gamma_s t}\sin\phi_s\sin(\Delta M_s t), \tag{16}$$

where we have introduced the abbreviation $\mathcal{N}_f \equiv (1-\lambda^2/2)\mathcal{A}'_f$, and ϕ_s is the CP-violating B_s^0–$\bar{B}_s^0$ mixing phase. In the ratio of the CP-violating rate difference (16), which requires the "tagging" of whether we had an initially, i.e. at time $t=0$, present B_s^0 or $\bar{B}_s^0$ meson, and the "untagged" rate (15), the overall normalization $|\mathcal{N}_f|$ cancels, so that ϕ_s can be extracted. For the corresponding time-dependences of the other observables provided by the angular distribution, see Ref. [2].

In the SM, we have $\phi_s^{\rm SM} = -2\lambda^2\eta = -(2.12\pm0.11)^\circ$, where the numerical value follows from the current CKM fits [14]. However, since B_s^0–$\bar{B}_s^0$ mixing is a strongly suppressed flavour-changing neutral-current (FCNC) process in the SM, it is a sensitive probe for NP effects in the TeV regime. Should new particles actually contribute to this phenomenon, the off-diagonal mass element of the mixing matrix is modified as follows [3]:

$$M_{12}^s = M_{12}^{s,{\rm SM}}\left(1+\kappa_s e^{i\sigma_s}\right), \tag{17}$$

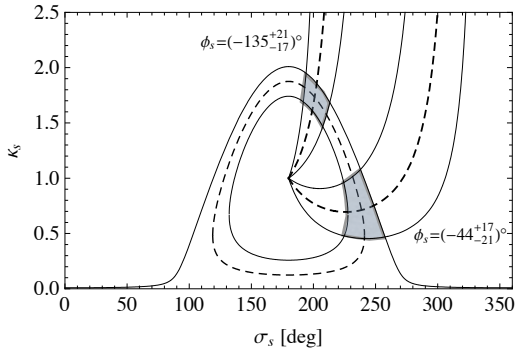

Figure 2: The situation in the σ_s–κ_s plane of the NP parameters for B_s^0–$\bar{B}_s^0$ mixing arising from current data and theory input, as discussed in the text.

where κ_s measures the strength of the NP contribution with respect to the SM, and σ_s is a CP-violating NP phase. Consequently, we have

$$\Delta M_s = \Delta M_s^{\rm SM} \left|1 + \kappa_s e^{i\sigma_s}\right|, \tag{18}$$

$$\phi_s = \phi_s^{\rm SM} + \phi_s^{\rm NP} = -2\lambda^2\eta + \arg(1 + \kappa_s e^{i\sigma_s}). \tag{19}$$

As discussed in Ref. [3], the values of $\rho_s \equiv \Delta M_s/\Delta M_s^{\rm SM}$ and $\phi_s^{\rm NP}$ can be converted into contours in the σ_s–κ_s plane, which sets the parameter space for NP contributions to B_s^0–$\bar{B}_s^0$ mixing.

For many years, only lower bounds on ΔM_s were available from the LEP (CERN) experiments and SLD (SLAC) [15]. In 2006, the value of ΔM_s could eventually be pinned down at the Tevatron [16]. The current status can be summarized as follows:

$$\Delta M_s = \begin{cases} (18.56 \pm 0.87)\text{ps}^{-1} & (\text{D}\emptyset \text{ collaboration [17]}), \\ (17.77 \pm 0.10 \pm 0.07)\text{ps}^{-1} & (\text{CDF collaboration [18]}). \end{cases} \tag{20}$$

In order to determine the parameter ρ_s from these measurements, the SM value of ΔM_s is required, involving a hadronic parameter $f_{B_s}^2 \hat{B}_{B_s}$, which can be determined by means of lattice QCD techniques and introduces the corresponding uncertainties into the analysis. The HPQCD collaboration finds $\Delta M_s^{\rm SM} = 20.3(3.0)(0.8)\,\text{ps}^{-1}$ [19], which yields $\rho_s = 0.88 \pm 0.13$.

Recently, following Refs. [1, 2], the CDF [4] and D$\emptyset$ [5] collaborations have reported the first results from tagged, time-dependent analyses of the full three-angle distribution of the $B_s^0 \to J/\psi[\to \ell^+\ell^-]\phi[\to K^+K^-]$ decay products. In an analysis by the UTfit collaboration [6], taking also other constraints into account, it is argued that these results may indicate CP-violating NP contributions to B_s^0–$\bar{B}_s^0$ mixing, which would immediately rule

out models with minimal flavour violation (MFV). Recently, a first average of the CDF and DØ data was presented by the Heavy Flavour Averaging Group (HFAG) [20], corresponding to the following twofold solution:

$$\phi_s = \left(-44^{+17}_{-21}\right)^\circ \vee \left(-135^{+21}_{-17}\right)^\circ . \tag{21}$$

In Fig. 2, we show – as an update of the analysis performed in Ref. [3] – the corresponding situation in the σ_s–κ_s plane: the central hill-like region corresponds to ρ_s, i.e. the mass difference ΔM_s, while the two branches represent the twofold solution for ϕ_s; the overlap of the ΔM_s and ϕ_s constraints results in the two shaded allowed regions. It will be very interesting to monitor these measurements in the future. Fortunately, the $B_s^0 \to J/\psi\phi$ analyses are very accessible at the LHCb experiment [7], which will soon start taking data.

2.4 Impact of Penguin Contributions

The experimental results discussed in the previous section were obtained by assuming that the doubly Cabibbo-suppressed parameters $a_f e^{i\theta_f}$, which describe – sloppily speaking – the ratio of penguin to tree contributions, play a negligible rôle. In view of the search for NP signals, which requires a solid control of the SM effects, and the tremendous accuracy that can be achieved at LHCb, we generalize here the formulae to take also these contributions into account.

Let us first have a look at the untagged observables. Following Ref. [13], we have

$$\begin{aligned} R_{\rm L}^f &= |\mathcal{N}_f|^2\Big[(1+\eta_f\cos\phi_s) \\ &\quad +2\epsilon a_f\cos\theta_f\left\{\cos\gamma+\eta_f\cos(\phi_s+\gamma)\right\}+\epsilon^2 a_f^2\left\{1+\eta_f\cos(\phi_s+2\gamma)\right\}\Big], \end{aligned} \tag{22}$$

$$\begin{aligned} R_{\rm H}^f &= |\mathcal{N}_f|^2\Big[(1-\eta_f\cos\phi_s) \\ &\quad +2\epsilon a_f\cos\theta_f\left\{\cos\gamma-\eta_f\cos(\phi_s+\gamma)\right\}+\epsilon^2 a_f^2\left\{1-\eta_f\cos(\phi_s+2\gamma)\right\}\Big], \end{aligned} \tag{23}$$

so that

$$\Gamma[f,t=0] = R_{\rm L}^f + R_{\rm H}^f = 2|\mathcal{N}_f|^2\Big[1+2\epsilon a_f\cos\theta_f\cos\gamma+\epsilon^2 a_f^2\Big]. \tag{24}$$

On the other hand, the CP-violating observables are given as follows:

$$A_{\rm D}^f = -2|\mathcal{N}_f|^2\epsilon a_f\sin\theta_f\sin\gamma, \tag{25}$$

$$A_{\rm M}^f = \eta_f|\mathcal{N}_f|^2\left[\sin\phi_s+2\epsilon a_f\cos\theta_f\sin(\phi_s+\gamma)+\epsilon^2 a_f^2\sin(\phi_s+2\gamma)\right]. \tag{26}$$

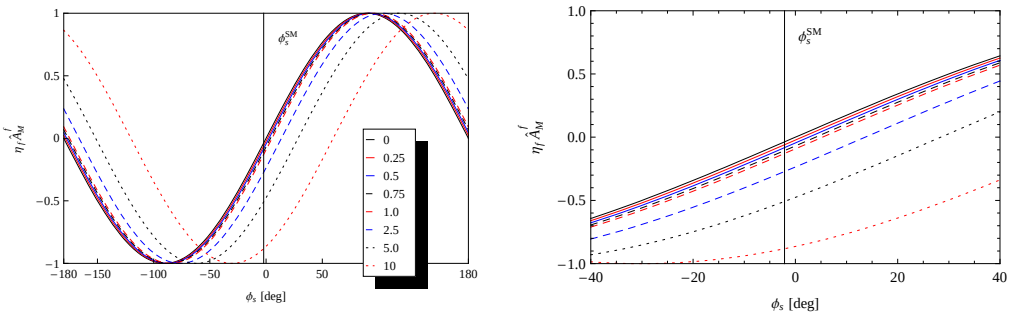

Figure 3: Impact of the penguin parameter a_f on the mixing-induced CP asymmetry $\eta_f \hat{A}_{\rm M}^f$ for $\theta_f = 180^\circ$ as function of the B_s^0–$\bar{B}_s^0$ mixing phase ϕ_s.

Note that (22) and (23) are not independent from (25) and (26), as

$$\left(A_{\rm D}^f\right)^2 + \left(A_{\rm M}^f\right)^2 = R_{\rm L}^f R_{\rm H}^f \,. \tag{27}$$

The ratio of the "tagged" rate difference (14) and the "untagged" rate (13) can be written as

$$\frac{|A_f(t)|^2 - |\overline{A}_f(t)|^2}{|A_f(t)|^2 + |\overline{A}_f(t)|^2} = \frac{\hat{A}_{\rm D}^f \cos(\Delta M_s t) + \hat{A}_{\rm M}^f \sin(\Delta M_s t)}{\cosh(\Delta\Gamma_s t/2) - \mathcal{A}_{\Delta\Gamma}^f \sinh(\Delta\Gamma_s t/2)}, \tag{28}$$

where $\Delta\Gamma_s \equiv \Gamma_{\rm H}^{(s)} - \Gamma_{\rm L}^{(s)}$, and

$$\mathcal{A}_{\Delta\Gamma}^f = \frac{R_{\rm H}^f - R_{\rm L}^f}{R_{\rm H}^f + R_{\rm L}^f}. \tag{29}$$

If we introduce

$$N_f \equiv 1 + 2\epsilon a_f \cos\theta_f \cos\gamma + \epsilon^2 a_f^2 = \frac{\Gamma[f, t=0]}{2|\mathcal{N}_f|^2}, \tag{30}$$

the corresponding observables take the following forms:

$$\hat{A}_{\rm D}^f = \frac{-2\epsilon a_f \sin\theta_f \sin\gamma}{N_f}, \tag{31}$$

$$\hat{A}_{\rm M}^f = +\frac{\eta_f}{N_f}\left[\sin\phi_s + 2\epsilon a_f \cos\theta_f \sin(\phi_s+\gamma) + \epsilon^2 a_f^2 \sin(\phi_s + 2\gamma)\right], \tag{32}$$

$$\mathcal{A}_{\Delta\Gamma}^f = -\frac{\eta_f}{N_f}\left[\cos\phi_s + 2\epsilon a_f \cos\theta_f \cos(\phi_s+\gamma) + \epsilon^2 a_f^2 \cos(\phi_s + 2\gamma)\right]. \tag{33}$$

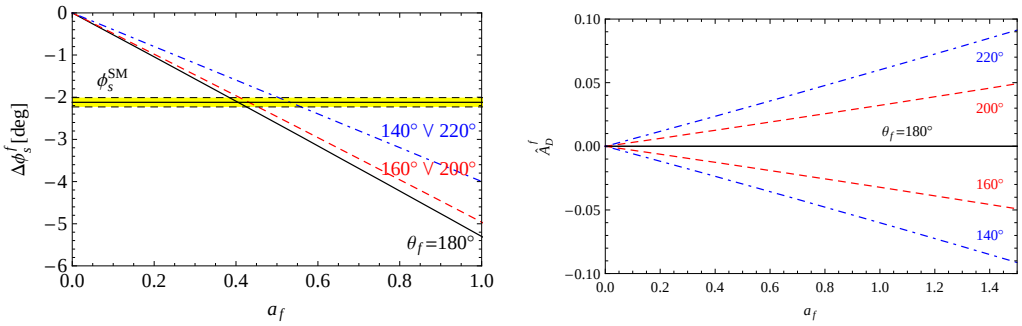

Figure 4: Left panel: the dependence of $\Delta\phi_s^f$ on a_f for various values of θ_f; right panel: the dependence of $\hat{A}_{\rm D}^f$ on a_f for various values of θ_f.

The measurement of $\mathcal{A}_{\Delta\Gamma}^f$ relies on a sizeable value of the width difference $\Delta\Gamma_s$. Moreover, we have

$$\left(\hat{A}_{\rm D}^f\right)^2 + \left(\hat{A}_{\rm M}^f\right)^2 + \left(\mathcal{A}_{\Delta\Gamma}^f\right)^2 = 1. \tag{34}$$

For the extraction of ϕ_s, the key observables are the $\hat{A}_{\rm M}^f$; in Fig. 3, we illustrate the impact of the penguin parameter a_f. Since $a_f e^{i\theta_f}$ is defined in (7) in such a way that θ_f is given by 180° if we assume factorization, we have used this value in order to calculate the curves shown in Fig. 3. For this strong phase the penguin effects are actually maximal in $\hat{A}_{\rm M}^f$ since only $\cos\theta_f$ enters. On the other hand, the direct CP asymmetries $\hat{A}_{\rm D}^f$ would then vanish, as they are proportional to $\sin\theta_f$.

We observe that in order to accommodate a value of $\phi_s \sim -44°$, as given in (21), we would need $a_f \sim 2.5$–5, which appears completely unrealistic. However, since a_f suffers from large uncertainties, values as large as $0.5 \sim 1$ can a priori not be excluded. Should ϕ_s take a value on the small side, these hadronic SM contributions would lead to a significant uncertainty in the extraction of the B_s^0–$\bar{B}_s^0$ mixing phase.

In order to explore this effect in more detail, we use (31) and (32) to derive the following expression:

$$\frac{\eta_f \hat{A}_{\rm M}^f}{\sqrt{1-(\hat{A}_{\rm D}^f)^2}} = \sin(\phi_s + \Delta\phi_s^f), \tag{35}$$

where

$$\sin\Delta\phi_s^f = \frac{2\epsilon a_f \cos\theta_f \sin\gamma + \epsilon^2 a_f^2 \sin 2\gamma}{N_f\sqrt{1-(\hat{A}_{\rm D}^f)^2}} \tag{36}$$

and

$$\cos\Delta\phi_s^f = \frac{1+2\epsilon a_f\cos\theta_f\cos\gamma+\epsilon^2 a_f^2\cos 2\gamma}{N_f\sqrt{1-(\hat{A}_{\rm D}^f)^2}}, \tag{37}$$

so that

$$\tan\Delta\phi_s^f = \frac{2\epsilon a_f\cos\theta_f\sin\gamma+\epsilon^2 a_f^2\sin 2\gamma}{1+2\epsilon a_f\cos\theta_f\cos\gamma+\epsilon^2 a_f^2\cos 2\gamma}. \tag{38}$$

It should be stressed that the shift $\Delta\phi_s^f$ of the B_s^0–$\bar{B}_s^0$ mixing phase does not depend on the value of ϕ_s itself. In Fig. 4, we show the dependence of $\Delta\phi_s^f$ on the penguin parameter a_f for various values of θ_f, and give – in order to monitor the corresponding direct CP asymmetries – a similar plot for $\hat{A}_{\rm D}^f$. We observe that $\Delta\phi_s^f$ is of the same size as $\phi_s^{\rm SM}$ for $a_f\sim 0.4$, and that a value of $a_f\sim 1$ would induce a shift of $\Delta\phi_s^f\sim -5^\circ$. As can be seen in the left panel of Fig. 4, we have $-0.05\lesssim\hat{A}_{\rm D}^f\lesssim+0.05$ for $a_f\lesssim 1$ and values of $|\theta_f-180^\circ|$ as large as 40°. Interestingly, as we expect $\cos\theta_f<0$, the shift of ϕ_s is expected to be negative as well, i.e. it would interfere constructively with $\phi_s^{\rm SM}$. These features are fully supported by our recent analysis of the $B^0\to J/\psi\pi^0$ channel [9]. Consequently, it is important to get a handle on the penguin effects in the $B_s^0\to J/\psi\phi$ decay.

3 The Control Channel $B_s^0\to J/\psi\bar{K}^{*0}$

3.1 Structure of the Decay Amplitudes

In Fig. 5, we show the decay topologies contributing to the $B_s^0\to J/\psi\bar{K}^{*0}$ channel. The key difference with respect to the $B_s^0\to J/\psi\phi$ decay shown in Fig. 1 is that $B_s^0\to J/\psi\bar{K}^{*0}$ is caused by $\bar{b}\to\bar{d}c\bar{c}$ quark-level processes, whereas $B_s^0\to J/\psi\phi$ originates from $\bar{b}\to\bar{s}c\bar{c}$ transitions. Consequently, the CKM factors are different in these channels. In analogy to (5), we may write

$$A(B_s^0\to(J/\psi\bar{K}^{*0})_f) = \lambda\mathcal{A}_f'\left[1-a_f' e^{i\theta_f'}e^{i\gamma}\right], \tag{39}$$

where $\mathcal{A}_f'$ and $a_f' e^{i\theta_f'}$ are the counterparts of the $B_s^0\to(J/\psi\phi)_f$ parameters introduced in (6) and (7), respectively. In contrast to (5), the latter parameter does *not* enter (39) in a doubly Cabibbo-suppressed way. Consequently, the $B_s^0\to J/\psi\bar{K}^{*0}$ channel offers a sensitive probe for this quantity. If we apply the $SU(3)$ flavour symmetry of strong interactions, we obtain

$$|\mathcal{A}_f| = |\mathcal{A}_f'|, \tag{40}$$

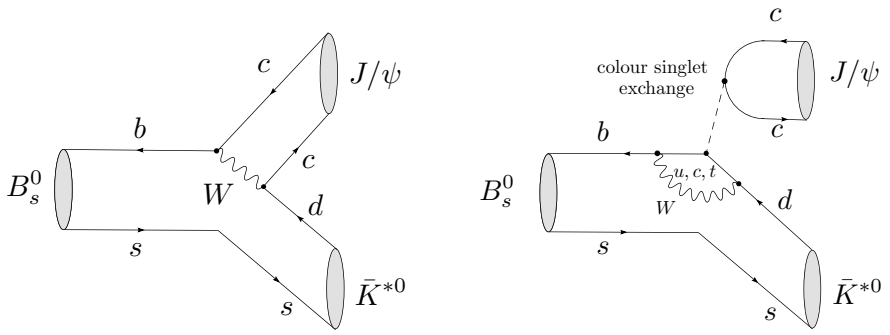

Figure 5: Decay topologies contributing to $B_s^0 \to J/\psi \bar{K}^{*0}$ in the SM.

as well as

$$a_f = a'_f, \quad \theta_f = \theta'_f. \tag{41}$$

In addition to $SU(3)$ flavour-symmetry arguments we have here also assumed that penguin annihilation (PA) and exchange (E) topologies, which contribute to $B_s^0 \to (J/\psi\phi)_f$ but have no counterpart in $B_s^0 \to J/\psi\bar{K}^{*0}$, play a negligible rôle. Fortunately, the importance of these topologies can be probed with the help of the $B_d^0 \to (J/\psi\phi)_f$ channel, which has amplitudes proportional to $(PA + E)_f$. The Belle collaboration has recently reported the new upper bound of $\mathrm{BR}(B_d^0 \to J/\psi\phi) < 9.4 \times 10^{-7}$ (90% C.L.) [21], which does not show any anomalous enhancement. The theoretical uncertainties associated with the application of the $SU(3)$ flavour symmetry will be discussed separately in Section 5.

3.2 Observables

In contrast to the $B_s^0 \to J/\psi[\to \ell^+\ell^-]\phi[\to K^+K^-]$ decay, the final states of $B_s^0 \to J/\psi[\to \ell^+\ell^-]\bar{K}^{*0}[\to \pi^+K^-]$ and its CP conjugate are flavour-specific, i.e. the charges of the pions and kaons depend on whether we had a B_s^0 or $\bar{B}_s^0$ meson in the initial state. Consequently, the time-dependent angular distributions do not show CP violation due to interference between mixing and decay, i.e. the A_{M}^f observables introduced in (14) have no counterparts, and do not depend on the B_s^0–$\bar{B}_s^0$ mixing phase. However, untagged observables, as well as direct CP-violating asymmetries provide actually sufficient information to determine a'_f and θ'_f. In Appendix A, we give the expressions for the time-dependent angular distributions, which allow the determination of the relevant observables.

Let us first discuss the untagged case, and introduce

$$H_f \equiv \frac{1}{\epsilon}\left|\frac{\mathcal{A}_f}{\mathcal{A}'_f}\right|^2 \frac{\Gamma[f,t=0]'}{\Gamma[f,t=0]} = \frac{1-2a'_f\cos\theta'_f\cos\gamma+a'^2_f}{1+2\epsilon a_f\cos\theta_f\cos\gamma+\epsilon^2 a_f^2}, \tag{42}$$

where $\Gamma[f,t=0]'$ is the $B_s^0 \to J/\psi\bar{K}^{*0}$ counterpart of (24). Using (40), we may extract H_f from the untagged observables. Moreover, using also (41), we can determine a'_f as a function of θ'_f with the help of the following formulae:

$$a'_f = U_{H_f} \pm \sqrt{U_{H_f}^2 - V_{H_f}}, \tag{43}$$

where

$$U_{H_f} \equiv \left(\frac{1+\epsilon H_f}{1-\epsilon^2 H_f}\right)\cos\theta'_f\cos\gamma, \tag{44}$$

and

$$V_{H_f} \equiv \frac{1-H_f}{1-\epsilon^2 H_f}. \tag{45}$$

Here the main uncertainty is associated with the determination of H_f, which relies on (40). In Subsection 5.2, we have a closer look at the corresponding $SU(3)$-breaking corrections, and give numerical results for the extraction of the H_f from the untagged observables. On the other hand, thanks to the ϵ terms in (42), the impact of corrections to (41) is tiny.

Another useful quantity is offered by the direct CP asymmetry

$$\hat{A}_{\rm D}^{f'} = \frac{2a'_f\sin\theta'_f\sin\gamma}{1-2a'_f\cos\theta'_f\cos\gamma+a'^2_f}, \tag{46}$$

which can be extracted from a rate difference; it takes the same form as (28) for $t=0$. In analogy to H_f, also $\hat{A}_{\rm D}^{f'}$ allows us to determine a'_f as a function of θ'_f. To this end, we may again use (43), with the following replacements:

$$U_{H_f} \;\to\; U_{\hat{A}_{\rm D}^{f'}} \equiv \cos\theta'_f\cos\gamma + \frac{\sin\theta'_f\sin\gamma}{\hat{A}_{\rm D}^{f'}}, \quad V_{H_f} \;\to\; V_{\hat{A}_{\rm D}^{f'}} \equiv 1. \tag{47}$$

It should be emphasized that the corresponding curve in the θ'_f–a'_f plane is theoretically clean, whereas that described by (43) is affected in particular by the $SU(3)$-breaking effects entering the determination of H_f.

The intersection of the H_f and $\hat{A}_{\rm D}^{f'}$ contours allows us then to extract a'_f and θ'_f from the data. Finally, applying (41) and the results derived in Section 2.4, we can include the penguin effects in the determination of the B_s^0–$\bar{B}_s^0$ mixing phase. Let us first illustrate this method in the next section by discussing a numerical example before giving a detailed discussion of the relevant $SU(3)$-breaking effects in Section 5.

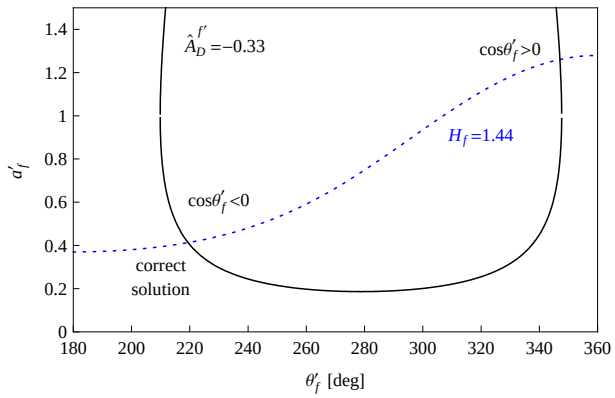

Figure 6: Illustration of the contours in the θ'_f–a'_f plane for an example, as discussed in the text.

4 A Numerical Example

For the illustration of the strategy discussed above, we assume $\gamma = 65°$, and hadronic parameters given by $a'_f = 0.4$ and $\theta'_f = 220°$, yielding the observables $H_f = 1.44$ and $\hat{A}_{\rm D}^{f'} = -0.33$. These input values are consistent with the ranges of the $B^0_d \to J/\psi\pi^0$ parameters $a' \in [0.15, 0.67]$ and $\theta' \in [174°, 213°]$ found in Ref. [9]; we expect a picture for a'_f and θ'_f that is similar to the one for their $B^0_d \to J/\psi\pi^0$ counterparts.

In Fig. 6, we show the contours in the θ'_f–a'_f plane that arise in this example. We observe that a twofold solution emerges for (θ'_f, a'_f), which can be resolved through the sign of $\cos\theta'_f$. Theoretically, we expect a negative value of this quantity, which is also supported by the $B^0_d \to J/\psi\pi^0$ data. In order to resolve this ambiguity experimentally, we need an additional observable, which would be provided by mixing-induced CP violation. Since the $B^0_s \to J/\psi[\to \ell^+\ell^-]\bar{K}^{*0}[\to \pi^+K^-]$ processes have flavour-specific final states, they do not show this phenomenon. On the other hand, mixing-induced CP violation would arise in $B^0_s \to J/\psi[\to \ell^+\ell^-]\bar{K}^{*0}[\to \pi^0 K_{\rm S,L}]$ modes, in analogy to $B^0_d \to J/\psi[\to \ell^+\ell^-]\bar{K}^{*0}[\to \pi^0 K_{\rm S,L}]$ processes [1]. Unfortunately, it is essentially impossible to study the corresponding experimental signatures in a hadronic environment, i.e. at the Tevatron or LHC.

However, we may alternatively use the $B^0_d \to J/\psi\rho^0$ channel [13], which can be obtained from $B^0_s \to J/\psi\bar{K}^{*0}$ by replacing the strange spectator quark through a down quark, as can be seen in Fig. 5. In this case, the final state is an admixture of different CP eigenstates, in analogy to $B^0_s \to J/\psi\phi$, and we can extract the following mixing-induced CP asymmetry from the time-

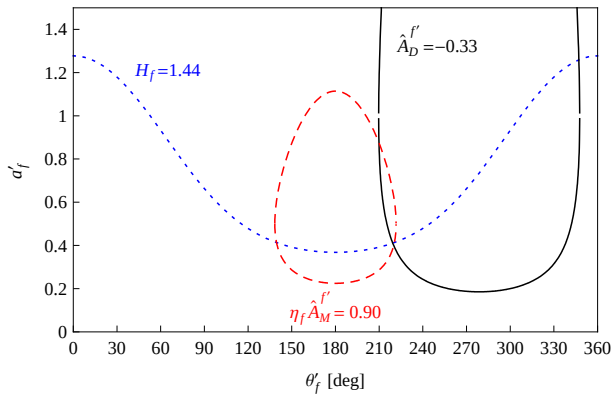

Figure 7: Illustration of the resolution of the twofold ambiguity in Fig. 6 through the mixing-induced CP violation in $B_d^0 \to J/\psi\rho^0$.

dependent angular distribution:

$$\hat{A}_{\rm M}^{f'} = +\eta_f \left[\frac{\sin\phi_d - 2a'_f\cos\theta'_f\sin(\phi_d+\gamma) + a'^2_f\sin(\phi_d+2\gamma)}{1 - 2a'_f\cos\theta'_f\cos\gamma + a'^2_f}\right], \tag{48}$$

where η_f is the CP eigenvalue of the final-state configuration f, i.e., η_0, $\eta_\parallel = +1$ and $\eta_\perp = -1$, whereas $\phi_d = (42.4^{+3.4}_{-1.7})^\circ$ denotes the B_d^0–$\bar{B}_d^0$ mixing phase [9]; for simplicity, we have also denoted the $B_d^0 \to J/\psi\rho^0$ hadronic parameters by a'_f and θ'_f, as we expect them to be approximately equal to those of $B_s^0 \to J/\psi\bar{K}^{*0}$ thanks to the $SU(3)$ flavour symmetry. Using (43) with the replacements

$$U_{H_f} \to U_{\hat{A}_{\rm M}^{f'}} \equiv \left[\frac{\sin(\phi_d+\gamma) - \hat{A}_{\rm M}^{f'}\cos\gamma}{\sin(\phi_d+2\gamma) - \hat{A}_{\rm M}^{f'}}\right]\cos\theta', \tag{49}$$

$$V_{H_f} \to V_{\hat{A}_{\rm M}^{f'}} \equiv \frac{\sin\phi_d - \hat{A}_{\rm M}^{f'}}{\sin(\phi_d+2\gamma) - \hat{A}_{\rm M}^{f'}}, \tag{50}$$

the measurement of the mixing-induced CP asymmetry $\hat{A}_{\rm M}^{f'}$ allows us to fix another contour in the θ'_f–a'_f plane. If we consider the example given above with $\phi_d = 42.4^\circ$, we obtain $\eta_f\hat{A}_{\rm M}^{f'} = 0.90$, which results in the contours shown in Fig. 7. We see that the twofold ambiguity in the determination of the hadronic parameters can now be resolved, thereby leaving us with our input values.

Since the width of the ρ^0 is three-times larger than that of the $\bar{K}^{*0}$, the $B_s^0 \to J/\psi\bar{K}^{*0}$ control channel should be experimentally better accessible than $B_d^0 \to J/\psi\rho^0$. Moreover, if we neglect $SU(3)$-breaking effects due to the different spectator quarks, we expect the simple relation

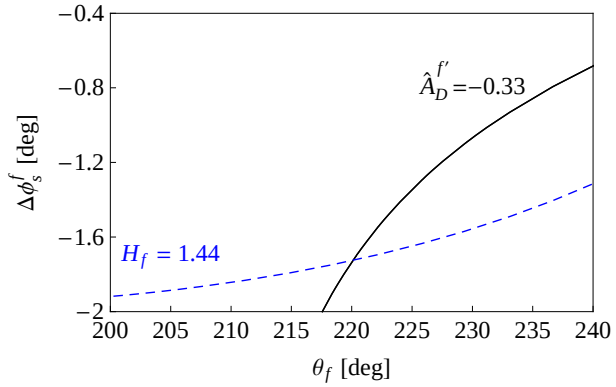

Figure 8: Situation in the θ_f–$\Delta\phi_s^f$ plane for the example in Figs. 6 and 7.

$\mathrm{BR}(B_s^0 \to J/\psi \bar{K}^{*0}) \sim 2 \times \mathrm{BR}(B_d^0 \to J/\psi\rho^0) = (4.6 \pm 0.4) \times 10^{-5}$ [20]. However, already a rather crude measurement of the mixing-induced CP-violating observables of $B_d^0 \to J/\psi\rho^0$ would be sufficient to resolve the ambiguity in the extraction of a'_f and θ'_f. In particular, the expected negative value of $\cos\theta'_f$ would be indicated by values of $\eta_f \hat{A}_{\rm M}^{f'}$ that are larger than $\sin\phi_d = 0.67$. Such a pattern emerges actually in the measurement of the mixing-induced CP violation of $B_d^0 \to J/\psi\pi^0$.

In Fig. 8, we convert the contours in the θ'_f–a'_f plane into the θ_f–$\Delta\phi_s^f$ space by means of (36)–(38) and (41). We observe that, in this specific example, the shift of the B_s^0 –$\bar{B}_s^0$ mixing phase through the penguin effects is given by $\Delta\phi_s^f = -1.7^\circ$. If we assume the SM, the mixing-induced CP asymmetries of $B_s^0 \to J/\psi\phi$ represented by (35) would be given by $\eta_f \hat{A}_{\rm M}^f = -6.7\%$, which is about twice as large as the SM value. At LHCb, such CP asymmetries could be detected with about $4\,\sigma$ significance after collecting $2\,\mathrm{fb}^{-1}$ of data, corresponding to one nominal year of operation, and with about $20\,\sigma$ at an upgrade of this experiment with $100\,\mathrm{fb}^{-1}$ integrated luminosity. However, without the control of the hadronic penguin effects through a simultaneous analysis of the $B_s^0 \to J/\psi \bar{K}^{*0}$ channel as proposed above, this result would be misinterpreted as a signal of physics beyond the SM. In this context it is important to emphasize that we expect $\phi_s^{\rm SM}$ and $\Delta\phi_s^f$ to have the same negative sign, thereby leading to constructive interference. In the opposite case, i.e. with a positive value of $\Delta\phi_s^f$, the SM picture of expecting vanishingly small CP violation in $B_s^0 \to J/\psi\phi$ would be much more robust with respect to the hadronic penguin uncertainties. It cannot be excluded that the hadronic penguin effects are actually more significant than in our example, and could lead to $\eta_f \hat{A}_{\rm M}^f \sim -10\%$. This feature is fully supported by the picture emerging from the current $B_d^0 \to J/\psi\pi^0$ data [9].

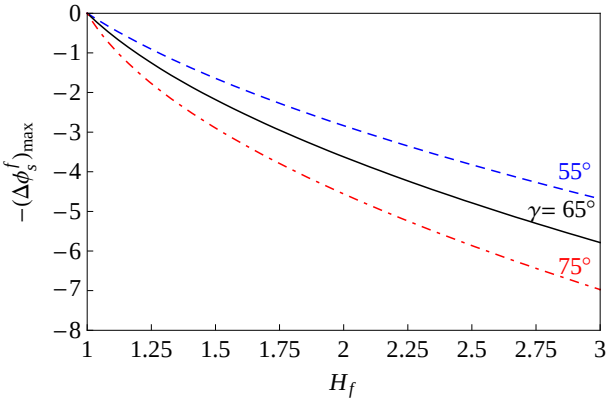

Figure 9: The maximal shift of ϕ_s as function of H_f for various values of γ.

In view of these findings, it would be very desirable to search for the $B_s^0 \to J/\psi \bar{K}^{*0}$ decay at the Tevatron. Already information on H_f would allow us to put first valuable constraints on the shift $\Delta\phi_s^f$. As we have shown in Fig. 9, these observables will put a first upper bound on $\Delta\phi_s^f$. Once direct CP violation in the $B_s^0 \to J/\psi \bar{K}^{*0}$ angular distribution is measured, $\Delta\phi_s^f$ can be fully pinned down, as we have shown above.

5 $SU(3)$-Breaking Effects

5.1 General Remarks and ω–ϕ Mixing

The main theoretical uncertainty of the strategy proposed in the present paper is related to $SU(3)$-breaking effects which affect the relations in (40) and (41). The following discussion of $SU(3)$ breaking is parallel to our previous investigation [9]; however, here we deal with vector meson final states. On the one hand this simplifies the discussion since $SU(3)$-breaking effects in the vector meson octett seem to be smaller; on the other hand, we have a ϕ state which is believed to be to a good approxmation an $\bar{s}s$ state and hence a superposition of $SU(3)$ eigenstates.

The $SU(3)$ nonet contains three neutral, non-strange states. Assuming isospin to be a good symmetry, one of these states is the neutral $I = 1$ ρ meson with the quark decomposition $\rho_0 = (u\bar{u} - d\bar{d})/\sqrt{2}$. The other two states are isosinglets and are given by $\phi_0 = (u\bar{u} + d\bar{d} + s\bar{s})/\sqrt{3}$, which is an $SU(3)$ singlet, and $\phi_8 = (u\bar{u} + d\bar{d} - 2s\bar{s})/4$ belonging to the $SU(3)$ octet. In case of unbroken $SU(3)$ symmetry, the amplitudes for processes involving the members of the octet are related to one another, while the singlet remains separate.

However, there is good indiction that the physical ϕ state is to a good approximation a pure $s\bar{s}$ state and hence a superposition of the singlet ϕ_0 and the octet ϕ_8. The orthogonal state $\omega = (u\bar{u} + d\bar{d})/\sqrt{2}$ is the isoscalar ω meson. Up to small mixing between ω and ϕ, which has been discussed recently in the context of B decays in Ref. [22], and which is too small to be relevant here, these are the (strong) mass eigenstates.

The way we apply the $SU(3)$ symmetry is to assume that the matrix elements of $\phi = s\bar{s}$ are related to the corresponding matrix elements of the members of the octet. In other words, we shall assume that the form factors of the $B_s^0 \to \phi$ transition are the same as the ones for the $B_s^0 \to \bar{K}^{*0}$ decay. Strictly speaking, this goes beyond the $SU(3)$ symmetry assumption since we relate octet and singlet components. Lacking any detailed information on the quality of such an asumption we have to rely, e.g., on QCD sum rule estimates which indicate that the strong dynamics in the $\phi = (s\bar{s})_{S=1}$ state are very similar to $K^{*0} = (d\bar{s})_{S=1}$; in fact, we shall rely on QCD sum rules in Section 5.2 to discuss the deviations from our assumption. In this context, it should be emphasized again that we have also to neglect penguin annihilation and exchange topologies, which can be probed through the $B_d^0 \to J/\psi\phi$ decay.

In a recent paper [23], it is argued in detail that the relations between $B_s^0 \to J/\psi\phi$ and $B_d^0 \to J/\psi K^{*0}$ following from flavour symmetry [24] are likely to be quite reliable, so that using strong phase information from the $B_d^0 \to J/\psi K^{*0}$ channel in the analysis of $B_s^0 \to J/\psi\phi$ is justified. Also here we have to assume that the matrix elements of $\phi = s\bar{s}$ are related to the corresponding matrix elements of the members of the octet.

It is very difficult to get a reliable estimate of the $SU(3)$ breaking for the non-leptonic decays at hand. It is known from the corresponding processes with pseudoscalar final states that the decays with J/ψ in the final state are dominated by non-factorizable contributions; it is not even clear how to factorize the penguin contributions in the decays we are considering. However, in the case of $B_{(s)} \to \pi\pi, \pi K, KK$ decays, we encounter sizeable non-factorizable effects, whereas the data do not indicate large $SU(3)$-breaking effects of this kind [25]. In particular, considering the counterpart of the H_f quantities introduced in the present paper for the $B_s^0 \to K^+K^-$, $B_d^0 \to \pi^+\pi^-$ system, a calculation of the relevant form-factor ratio by means of QCD sum rule techniques [26] yields good agreement with the current data that would be spoiled by large non-factorizable, $SU(3)$-breaking effects.

This empirical behaviour gives us conficence that our estimate of the $SU(3)$-breaking effects for the extraction of the H_f from the data given in the next subsection, which relies on a QCD sum rule analysis of the relevant form factors as well, describes the leading corrections.

5.2 $SU(3)$ Breaking in the Extraction of H_f

In order to calculate the $SU(3)$-breaking corrections to the amplitude ratios $|\mathcal{A}_f/\mathcal{A}'_f|$ that are required for the extraction of the H_f from the data (see (42)), we apply the formulae given in Ref. [1]. The linear polarization amplitudes of the $B_s^0 \to J/\psi\phi$ channel at time $t = 0$ can be written as

$$\begin{aligned} A_0(0) &= -xa - (x^2-1)b \\ A_\parallel(0) &= \sqrt{2}a \\ A_\perp(0) &= \sqrt{2(x^2-1)}\; c \end{aligned} \tag{51}$$

with

$$x \equiv \frac{p_{J/\psi}\cdot p_\phi}{m_{J/\psi}m_\phi} = \frac{m_{B_s}^2 - m_{J/\psi}^2 - m_\phi^2}{2m_{J/\psi}m_\phi}, \tag{52}$$

where the "factorized" contributions are given by

$$\begin{aligned} a_{\rm fact} &= \frac{G_{\rm F}}{\sqrt{2}}\lambda_c^{(s)}\big(\mathcal{C}_1^{\rm eff}(\mu) + \mathcal{C}_5^{\rm eff}(\mu)\big)A_1^{\rm fact}\;, \\ b_{\rm fact} &= \frac{G_{\rm F}}{\sqrt{2}}\lambda_c^{(s)}\big(\mathcal{C}_1^{\rm eff}(\mu) + \mathcal{C}_5^{\rm eff}(\mu)\big)B_1^{\rm fact}, \\ c_{\rm fact} &= \frac{G_{\rm F}}{\sqrt{2}}\lambda_c^{(s)}\big(\mathcal{C}_1^{\rm eff}(\mu) + \mathcal{C}_5^{\rm eff}(\mu)\big)C_1^{\rm fact}. \end{aligned} \tag{53}$$

Here we have neglected the doubly Cabibbo-suppressed penguin corrections, as our target are the overall amplitudes $\mathcal{A}_f$; $G_{\rm F}$ is Fermi's constant, $\lambda_c^{(s)}$ the CKM factor introduced after (4), and the $\mathcal{C}_i^{\rm eff}(\mu)$ are the "effective" Wilson coefficient functions introduced in Ref. [1]. Moreover, we have

$$\begin{aligned} A_1^{\rm fact} &= -f_{J/\psi}m_{J/\psi}(m_{B_s}+m_\phi)A_1^{B_s\phi}(m_{J/\psi}^2)\;, \\ B_1^{\rm fact} &= 2\,\frac{f_{J/\psi}m_{J/\psi}^2 m_\phi}{m_{B_s}+m_\phi}\;A_2^{B_s\phi}(m_{J/\psi}^2)\;, \\ C_1^{\rm fact} &= 2\,\frac{f_{J/\psi}m_{J/\psi}^2 m_\phi}{m_{B_s}+m_\phi}\;V^{B_s\phi}(m_{J/\psi}^2), \end{aligned} \tag{54}$$

where $A_{1,2}^{B_s\phi}(q^2)$ and $V^{B_s\phi}(q^2)$ are the form factors of the quark-current matrix elements of the $B_s \to \phi$ transition, with q denoting the momentum transferred by the quark current. In the case of the $B_s^0 \to J/\psi\bar{K}^{*0}$ channel, we need correspondingly the $B_s \to \bar{K}^{*0}$ transition form factors, and have to replace $\phi \to \bar{K}^{*0}$ in (52) and (54).

An analysis of these form factors was performed in Ref. [27]. Light cone QCD sum rules allow an estimate of the values of the form factors at $q^2 =$

	$V=\phi$	$V=\bar{K}^*$
$A_1^{B_s\to V}(m^2_{J/\psi})$	0.42 ± 0.06	0.33 ± 0.05
$A_2^{B_s\to V}(m^2_{J/\psi})$	0.38 ± 0.06	0.32 ± 0.05
$V^{B_s\to V}(m^2_{J/\psi})$	$0.82\ \pm0.12$	0.62 ± 0.09

Table 1: Collection of the relevant $B_s\to V$ form factors at $q^2=m^2_{J/\psi}$, using the results of Ref. [27] and assuming an uncertainty of 15%.

0. In order to obtain the value of the form factor at a different q^2, such as $q^2=m^2_{J/\psi}$ as in (54), we have to make an extrapolation using some parametrization of the form factor. If we use the functional forms suggested in Ref. [27] and assume an uncertainty of 15%, we obtain the form factors at $q^2=m^2_{J/\psi}$ collected in Table 1, and the following $SU(3)$-breaking ratios:

$$\begin{aligned}\frac{A_1^{B_s\to\bar{K}^*}(m^2_{J/\psi})}{A_1^{B_s\to\phi}(m^2_{J/\psi})}&=0.78\pm0.08\ ,\\ \frac{A_2^{B_s\to\bar{K}^*}(m^2_{J/\psi})}{A_2^{B_s\to\phi}(m^2_{J/\psi})}&=0.84\pm0.07\ ,\\ \frac{V^{B_s\to\bar{K}^*}(m^2_{J/\psi})}{V^{B_s\to\phi}(m^2_{J/\psi})}&=0.76\pm0.15\ .\end{aligned}\tag{55}$$

Using then (51), we obtain the following numerical results, which allow the extraction of the H_f from the untagged rates with the help of (42):

$$\begin{aligned}\left|\frac{\mathcal{A}'_0}{\mathcal{A}_0}\right|^2&=0.42\pm0.27\ ,\\ \left|\frac{\mathcal{A}'_\parallel}{\mathcal{A}_\parallel}\right|^2&=0.70\pm0.29\ ,\\ \left|\frac{\mathcal{A}'_\perp}{\mathcal{A}_\perp}\right|^2&=0.38\pm0.16\ .\end{aligned}\tag{56}$$

Note that in order to calculate $|\mathcal{A}'_0/\mathcal{A}_0|^2$, we need the $A_{1,2}^{B_s\to V}(m^2_{J/\psi})$ form factors given in Table 1.

5.3 $SU(3)$ Breaking in $a'_f=a_f$ and $\theta'_f=\theta_f$

If we use the $B_s^0\to J/\psi\bar{K}^{*0}$ observables as discussed in Section 3, we can extract a'_f and θ'_f from the data. Since their $B_s^0\to J/\psi\phi$ counterparts a_f and

θ_f enter in H_f in combination with the tiny parameter ϵ, this determination is essentially unaffected by corrections to (41); the main corrections enter through the value of H_f, which requires the amplitude ratios $|\mathcal{A}_f/\mathcal{A}'_f|$, with the $SU(3)$-breaking corrections estimated in the previous subsection.

When calculating the shifts $\Delta\phi_s^f$, we have to use the relations in (41). However, one has to keep in mind that sizable non-factorizable effects could induce $SU(3)$-breaking corrections. Their impact on the determination of $\Delta\phi_s^f$ can be easily inferred from (38). Neglecting terms of order ϵ^2, we have a linear dependence on $a_f \cos\theta_f$. Consequently, corrections to the left-hand side of (41) propagate linearly, while $SU(3)$-breaking effects in the strong phases will generally lead to an asymmetric uncertainty for $\Delta\phi_s^f$.

In the analysis of the $B_d^0 \to J/\psi\pi^0$ data in Ref. [9], the impact of $SU(3)$-breaking corrections was explored by setting $a = \xi a'$ and uncorrelating the strong phases θ and θ' of the $B_d^0 \to J/\psi K^0$ and $B_d^0 \to J/\psi\pi^0$ decays, respectively. Even when allowing for $\xi \in [0.5, 1.5]$ and $\theta, \theta' \in [90, 270]^\circ$ in the corresponding fit, and using a 50% increased error for the relevant form-factor ratio to explore the impact of dramatic non-factorizable, $SU(3)$-breaking contributions to $|\mathcal{A}/\mathcal{A}'|$, the picture emerging from the global fit is not significantly changed. To be specific, $\Delta\phi_d \in [-6.7, 0.0]^\circ$ arises when allowing for such large $SU(3)$-breaking corrections, whereas $\Delta\phi_d \in [-3.9, -0.8]^\circ$ in the case with $\xi = 1$ and $\theta = \theta'$. We expect a similar situation for $\Delta\phi_s^f$.

5.4 Internal Consistency Checks of $SU(3)$

The advantage of B decays into two vector mesons is that many more observables are offered by the angular distribution of their decay products than in the case of $B \to PP$ or $B \to PV$ decays (P and V denote generically pseudoscalar and vector mesons, respectively). This comment applies also to the decays considered in the present paper, and allows us to perform internal consistency checks of the $SU(3)$ flavour symmetry.

A very first internal test follows from a comparison of the different values of the B_s^0–$\bar{B}_s^0$ mixing phase ϕ_s following from the three polarization states $f \in \{0, \|, \perp\}$. Obviously, these values should agree with one another. In fact, even more quantitative tests of $SU(3)$ breaking can be performed. The point is that we may choose one of the three linear polarization states to extract ϕ_s from (35), taking the shift $\Delta\phi_s^f$ through the penguin effects into account. Using then the $B_s^0 \to J/\psi\phi$ observables $\hat{A}_{\rm M}^f$ and $\hat{A}_{\rm M}^f$ of the remaining two polarization states, the knowledge of ϕ_s allows us to extract the corresponding shifts $\Delta\phi_s^f$ from (35). With the help of (38), we can then convert the values of the $\Delta\phi_s^f$ into contours in the θ_f–a_f plane. To this end, we have simply to

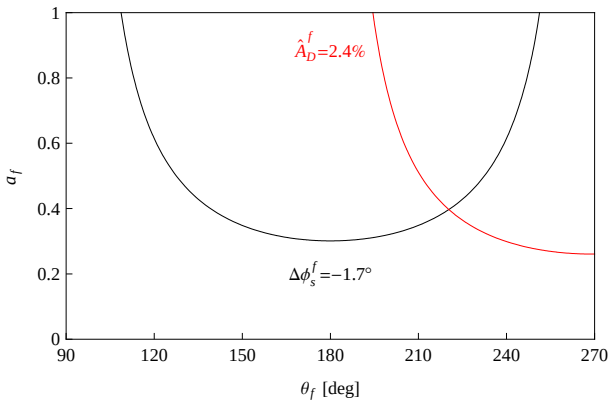

Figure 10: The extraction of a_f and θ_f from $\Delta\phi_s^f$ and the direct CP asymmetry $\hat{A}_{\rm D}^f$ for internal consistency checks of the $SU(3)$ flavour symmetry, as described in the text. The example corresponds to $a_f = 0.4$ and $\theta_f = 220°$ with $\gamma = 65°$, as in the previous numerical illustrations.

make the following replacements in (43):

$$U_{H_f} \to U_{\Delta\phi_s^f} \equiv \left(\frac{\sin\gamma - \cos\gamma\tan\Delta\phi_s^f}{\cos 2\gamma\tan\Delta\phi_s^f - \sin 2\gamma}\right)\cos\theta_f, \tag{57}$$

$$V_{H_f} \to V_{\Delta\phi_s^f} \equiv \frac{\tan\Delta\phi_s^f}{\cos 2\gamma\tan\Delta\phi_s^f - \sin 2\gamma}, \tag{58}$$

as well as $a_f' \to \epsilon a_f$. Moreover, if we replace, in addition to the latter substitution, $\theta_f' \to 180° + \theta_f$ and $\hat{A}_{\rm D}^{f'} \to \hat{A}_{\rm D}^f$ in (47), the direct CP asymmetry in $B_s^0 \to J/\psi\phi$ can be converted into a contour in the θ_f–a_f plane as well. It should be stressed that these constructions are valid exactly. In Fig. 10, we illustrate how this works by considering again the numerical example specified in Section 4.

The values of the hadronic $B_s^0 \to J/\psi\phi$ parameters a_f and θ_f allow us then to perform an internal consistency check of the $SU(3)$ flavour symmetry by comparing with the values of a_f' and θ_f' following from the $B_s^0 \to J/\psi\bar{K}^{*0}$ strategy proposed in Section 3. Another test is offered by the following relations:

$$\hat{A}_{\rm D}^f = -\epsilon H_f \hat{A}_{\rm D}^{f'}, \tag{59}$$

which rely on (41). Needless to note, the practical usefulness of these consistency checks depends on the values of the observables that will eventually be measured by LHCb. We strongly encourage detailed feasibility studies and look forward to confronting these considerations with real data soon.

6 Conclusions

Studies of CP-violating effects in the time-dependent angular distribution of $B_s^0 \to J/\psi[\to \ell^+\ell^-]\phi[\to K^+K^-]$ processes have recently received considerable attention in view of first tagged measurements at the Tevatron, and are a central target of the LHCb experiment which will soon start taking data. We have pointed out that hadronic effects, which are due to doubly Cabibbo-suppressed penguin contributions that are usually neglected, could induce mixing-induced CP-violating effects as large as $\mathcal{O}(-10\%)$. Without the control of these penguin contributions, which cannot be calcuated reliably from QCD, such CP-violating effects, which can be detected with excellent significance by LHCb, would be misinterpreted as CP-violating NP contributions to B_s^0–$\bar{B}_s^0$ mixing.

In the present paper, we have proposed a strategy to include these contributions with the help of a measurement of the angular distribution of the $B_s^0 \to J/\psi[\to \ell^+\ell^-]\bar{K}^{*0}[\to \pi^+K^-]$ decay products, and have illustrated this by means of a numerical example. We strongly suggest a search for this control channel at the Tevatron in order to obtain first constraints on the penguin effects in the $B_s^0 \to J/\psi\phi$ analysis. The tremendous accuracy that can be achieved at LHCb and a possible future upgrade of this experiment makes it mandatory to include these penguin contributions.

Acknowledgements: S.F. and T.M. acknowledge the support by the German Ministry of Research (BMBF, Contract No. 05HT6PSA), and R.F. would like to thank Guido Martinelli for the hospitality at the Università di Roma "La Sapienza".

Appendix

A Time-dependent Angular Distributions of $B_s^0 \to J/\psi \bar{K}^{*0}$ and CP Conjugates

Following Ref. [1], we introduce the following set of trigonometric functions:

$$\begin{array}{rcl} f_1 &=& 2\,\cos^2\psi\,(1-\sin^2\theta\,\cos^2\varphi) \\ f_2 &=& \sin^2\psi\,(1-\sin^2\theta\,\sin^2\varphi) \\ f_3 &=& \sin^2\psi\,\sin^2\theta \\ f_4 &=& \sin^2\psi\,\sin 2\theta\,\sin\varphi \\ f_5 &=& (1/\sqrt{2})\,\sin 2\psi\,\sin^2\theta\sin 2\varphi \\ f_6 &=& (1/\sqrt{2})\,\sin 2\psi\,\sin 2\theta\,\cos\varphi. \end{array} \tag{60}$$

If we use the notation $A_f \equiv A(B_s^0 \to (J/\psi \bar{K}^{*0})_f)$ for the unevolved amplitude in (39) and $\bar{A}_f$ for its CP conjugate, we obtain

$$\frac{d^3\Gamma[B_s^0(t) \to J/\psi(\to \ell^+\ell^-)\bar{K}^{*0}(\to \pi^+K^-)]}{d\cos\theta\; d\varphi\; d\cos\psi} = \frac{9}{64\pi}\,[\cosh(\Delta\Gamma_s t/2) + \cos(\Delta M_s t)]\,e^{-\Gamma_s t}$$
$$\times\left\{f_1|A_0|^2 + f_2|A_\parallel|^2 + f_3|A_\perp|^2 - f_4 Im\,(A_\parallel^* A_\perp) + f_5 Re\,(A_0^* A_\parallel) + f_6 Im\,(A_0^* A_\perp)\right\} \tag{61}$$

$$\frac{d^3\Gamma[\bar{B}_s^0(t) \to J/\psi(\to \ell^+\ell^-)K^{*0}(\to \pi^-K^+)]}{d\cos\theta\; d\varphi\; d\cos\psi} = \frac{9}{64\pi}\,[\cosh(\Delta\Gamma_s t/2) + \cos(\Delta M_s t)]\,e^{-\Gamma_s t}$$
$$\times\left\{f_1|\bar{A}_0|^2 + f_2|\bar{A}_\parallel|^2 + f_3|\bar{A}_\perp|^2 + f_4\,Im\,(\bar{A}_\parallel^* \bar{A}_\perp) + f_5\,Re\,(\bar{A}_0^* \bar{A}_\parallel) - f_6\,Im\,(\bar{A}_0^* \bar{A}_\perp)\right\} \tag{62}$$

$$\frac{d^3\Gamma[B_s^0(t) \to J/\psi(\to \ell^+\ell^-)K^{*0}(\to \pi^-K^+)]}{d\cos\theta\; d\varphi\; d\cos\psi} = \frac{9}{64\pi}\,[\cosh(\Delta\Gamma_s t/2) - \cos(\Delta M_s t)]\,e^{-\Gamma_s t}$$
$$\times\left\{f_1|\bar{A}_0|^2 + f_2|\bar{A}_\parallel|^2 + f_3|\bar{A}_\perp|^2 + f_4\,Im\,(\bar{A}_\parallel^* \bar{A}_\perp) + f_5\,Re\,(\bar{A}_0^* \bar{A}_\parallel) - f_6\,Im\,(\bar{A}_0^* \bar{A}_\perp)\right\} \tag{63}$$

$$\frac{d^3\Gamma[\bar{B}_s(t) \to J/\psi(\to \ell^+\ell^-)\bar{K}^{*0}(\to \pi^+K^-)]}{d\cos\theta\; d\varphi\; d\cos\psi} = \frac{9}{64\pi}\,[\cosh(\Delta\Gamma_s t/2) - \cos(\Delta M_s t)]\,e^{-\Gamma_s t}$$
$$\times\left\{f_1|A_0|^2 + f_2|A_\parallel|^2 + f_3|A_\perp|^2 - f_4\,Im\,(A_\parallel^* A_\perp) + f_5\,Re\,(A_0^* A_\parallel) + f_6\,Im\,(A_0^* A_\perp)\right\}. \tag{64}$$

In the case of $\Delta\Gamma_s \to 0$, we have

$$\cosh(\Delta\Gamma_s t/2) + \cos(\Delta M_s t) \to 2\cos^2(\Delta M_s t/2), \tag{65}$$

$$\cosh(\Delta\Gamma_s t/2) - \cos(\Delta M_s t) \to 2\sin^2(\Delta M_s t/2). \tag{66}$$

Consequently, the expressions listed above reduce to those given in Ref. [1] for the flavour-specific $B_d \to J/\psi[\to \ell^+\ell^-]K^*[\to K^\pm\pi^\mp]$ modes with the assumption of $|A_f| = |\bar{A}_f|$.

References

[1] A. S. Dighe, I. Dunietz and R. Fleischer, Eur. Phys. J. C **6**, 647 (1999) [arXiv:hep-ph/9804253].

[2] I. Dunietz, R. Fleischer and U. Nierste, Phys. Rev. D **63**, 114015 (2001) [arXiv:hep-ph/0012219].

[3] P. Ball and R. Fleischer, Eur. Phys. J. C **48**, 413 (2006) [arXiv:hep-ph/0604249].

[4] T. Aaltonen *et al.* [CDF Collaboration], Phys. Rev. Lett. **100**, 161802 (2008) [arXiv:0712.2397 [hep-ex]].

[5] V. M. Abazov *et al.* [DØ Collaboration], arXiv:0802.2255 [hep-ex].

[6] M. Bona *et al.* [UTfit Collaboration], arXiv:0803.0659 [hep-ph].

[7] O. Leroy [on behalf of the LHCb Collaboration], talk at CERN Theory Institute "Flavour as a Window to New Physics at the LHC", CERN, 5 May – 13 June, 2008 [http://ph-dep-th.web.cern.ch/ph-dep-th/content2/THInstitutes/2008/flavour/TH-Flavour.html].

[8] The LHCb Collaboration, *Expression of Interest for an LHCb Upgrade*, CERN/LHCC/2008-007.

[9] S. Faller, R. Fleischer, M. Jung and T. Mannel, arXiv:0809.0842 [hep-ph].

[10] M. Ciuchini, M. Pierini and L. Silvestrini, Phys. Rev. Lett. **95**, 221804 (2005).

[11] J. L. Rosner, Phys. Rev. D **42**, 3732 (1990).

[12] Particle Data Group, 2008 update, see http://pdg.lbl.gov/.

[13] R. Fleischer, Phys. Rev. D **60**, 073008 (1999) [arXiv:hep-ph/9903540].

[14] M. Bona *et al.* [UTfit Collaboration], JHEP **0507**, 028 (2005); for the most recent updates, see http://utfit.roma1.infn.it/.

[15] B Oscillations Working Group: `http://lepbosc.web.cern.ch/LEPBOSC/`.

[16] V.M. Abazov *et al.* [DØ Collaboration], Phys. Rev. Lett. **97**, 021802 (2006) [arXiv:hep-ex/0603029]; A. Abulencia *et al.* [CDF Collaboration], Phys. Rev. Lett. **97**, 062003 (2006) [arXiv:hep-ex/0606027].

[17] DØ Collaboration, DØnote 5474-conf (2007) [http://www-d0.fnal.gov].

[18] A. Abulencia *et al.* [CDF Collaboration], Phys. Rev. Lett. **97**, 242003 (2006) [arXiv:hep-ex/0609040].

[19] E. Dalgic *et al.* [HPQCD Collaboration], Phys. Rev. D **76**, 011501 (2007) [arXiv:hep-lat/0610104].

[20] E. Barberio *et al.* [Heavy Flavour Averaging Group], arXiv:0808.1297 [hep-ex]; for the most recent updates, see http://www.slac.stanford.edu/xorg/hfag.

[21] Y. Liu *et al.* [Belle Collaboration], Phys. Rev. D **78**, 011106 (2008) [arXiv:0805.3225 [hep-ex]].

[22] M. Gronau and J. L. Rosner, Phys. Lett. B **666**, 185 (2008) [arXiv:0806.3584 [hep-ph]].

[23] M. Gronau and J. L. Rosner, arXiv:0808.3761 [hep-ph].

[24] A. S. Dighe, I. Dunietz and R. Fleischer, Phys. Lett. B **433**, 147 (1998) [arXiv:hep-ph/9804254].

[25] R. Fleischer, Eur. Phys. J. C **52**, 267 (2007) [arXiv:0705.1121 [hep-ph]].

[26] A. Khodjamirian, T. Mannel and M. Melcher, Phys. Rev. D **70**, 094002 (2004) [arXiv:hep-ph/0407226].

[27] P. Ball and R. Zwicky, Phys. Rev. D **71**, 014029 (2005) [arXiv:hep-ph/0412079].